Journal of Asian Earth Sciences 111 (2015) 44–53

Contents lists available at ScienceDirect

Journal of Asian Earth Sciences

journal homepage: www.elsevier.com/locate/jseaes

Late Pliocene temperatures and their spatial variation at the southeastern border of the Qinghai–Tibet Plateau

Yong-Jiang Huang [a,c], Wen-Yun Chen [a], Frédéric M.B. Jacques [b], Yu-Sheng Christopher Liu [d], Torsten Utescher [e,f], Tao Su [b], David K. Ferguson [g], Zhe-Kun Zhou [a,b,*]

[a] Key Laboratory for Plant Biodiversity and Biogeography of East Asia, Kunming Institute of Botany, Chinese Academy of Sciences, Kunming 650201, China
[b] Key Laboratory of Tropical Forest Ecology, Xishuangbanna Tropical Botanical Garden, Chinese Academy of Sciences, Mengla 666303, China
[c] State Key Laboratory of Paleobiology and Stratigraphy, Nanjing Institute of Geology and Paleontology, Chinese Academy of Sciences, Nanjing 210008, China
[d] Department of Biological Sciences, East Tennessee State University, Johnson City, TN 37614-1730, USA
[e] Steinmann Institute, University of Bonn, Bonn, Germany
[f] Senckenberg Research Institute, Frankfurt am Main, Germany
[g] Institute of Palaeontology, University of Vienna, Althanstrasse 14, Vienna A-1090, Austria

ARTICLE INFO

Article history:
Received 14 February 2014
Received in revised form 1 April 2015
Accepted 29 April 2015
Available online 10 June 2015

Keywords:
Late Pliocene
Palaeoclimatic reconstruction
Temperature
Precipitation
Qinghai–Tibet Plateau
Coexistence Approach

ABSTRACT

It is widely accepted that the late Pliocene spans a time with globally warmer conditions compared to today. Regional specifics in temperature patterns from this period, however, remain poorly known. In this study, we reconstruct quantitatively late Pliocene climates for eight sites at the southeastern border of the Qinghai–Tibet Plateau (SBTP), based on palaeobotanical data compiled from published sources using the Coexistence Approach (CoA), and analyze anomalies with respect to modern climates. The reconstructed temperatures indicate that in the late Pliocene, the northwestern part of the study area was cooler than its southern part. This spatial differentiation in temperature was largely due to differences in altitude: the northwest of the SBTP probably had higher altitudes than the south at that time. Mean annual temperatures (MATs) were around 1 °C higher than today, suggesting a cooling trend since the late Pliocene. Our data show that summer temperatures have declined significantly since the late Pliocene while winter temperatures have remained similar to those of the present, different from observations in other territories. The unexpected summer and winter temperature changes can be explained by the regional orogenic uplift plus the global cooling. The eastward extrusion of the Qinghai–Tibet Plateau might have blocked the southward cold high pressure of the winter monsoon and forced it to circumvent the eastern flank of the plateau, weakening its impact on the SBTP. The post-Pliocene mountain uplift increased the overall altitude of the region, which caused the temperature decline for both summer and winter. The reconstructed summer precipitation was lower while the winter precipitation was higher than today, suggesting a weaker monsoon climate during the late Pliocene.

1. Introduction

The late Pliocene epoch spans a time when the Earth experienced a transition from warm conditions to the Pleistocene icehouse. Temperature reconstructions at the global scale consistently indicate a warmer late Pliocene compared to today (Zachos et al., 2001; Dowsett et al., 2009; Salzmann et al., 2011). Regional observations in temperature patterns from this time period, however, are not yet well known.

In recent years, the southeastern border of the Qinghai–Tibet Plateau (SBTP) has become the focus of several studies regarding its climates during the late Pliocene (Xu et al., 2004; Kou et al., 2006; Sun et al., 2011; Xie et al., 2012; Yao et al., 2012; Su et al., 2013). This region experienced dramatic changes in topography and climate throughout the late Cenozoic associated with the uplift and expansion of the Qinghai–Tibet Plateau (Kutzbach et al., 1993; Ge and Li, 1999; Schoenbohm et al., 2006; Westaway, 2009; Zhang et al., 2012). Eastward and southeastward extrusions of the Qinghai–Tibet Plateau occurred during the later stages of the Cenozoic, causing mountain uplift to the north of the SBTP (England and Houseman, 1989; Clark and Royden, 2000; Williams et al., 2001; Zhang and Ding, 2003; Shen et al., 2005; Westaway, 2009). Intense orogenic processes also triggered uplift

* Corresponding author at: Key Laboratory for Plant Biodiversity and Biogeography of East Asia, Kunming Institute of Botany, Chinese Academy of Sciences, 132# Lanhei Road, Kunming 650201, Yunnan, China. Tel./fax: +86 0871 65219932.
E-mail address: zhouzk@mail.kib.ac.cn (Z.-K. Zhou).

http://dx.doi.org/10.1016/j.jseaes.2015.04.048
1367-9120/© 2015 Elsevier Ltd. All rights reserved.

of various parts of the SBTP region itself since the Pliocene (Schoenbohm et al., 2004, 2006; Shen et al., 2005). Furthermore, the uplift of the Qinghai–Tibet Plateau had a huge impact on the surrounding atmospheric circulation and led to the establishment and intensification of the Asian monsoon climate in South and East China: summer rainfall increased while winter precipitation decreased (Zheng et al., 2004; Harris, 2006; Biasatti et al., 2010). The combination of mountain uplift and monsoon intensification makes the SBTP an interesting key region to study the regional climates of the late Pliocene.

The SBTP comprises a series of isolated sedimentary basins, many of which yield well-exposed Neogene sediments containing plant fossil remains (Ge and Li, 1999). Around 20 Neogene floras have been well documented from this region, of which several are late Pliocene in age (e.g., Tao, 1986; Ge and Li, 1999; Zhou, 2000; Xu, 2002; Xu et al., 2003, 2004; Wang and Shu, 2004; Kou et al., 2006; Su et al., 2013). During the last decade, palaeoclimate data for some of those late Pliocene floras were reconstructed quantitatively (Xu, 2002; Xu et al., 2004; Kou et al., 2006; Sun et al., 2011; Yao et al., 2012; Su et al., 2013). These palaeoclimatic reconstructions consistently show warmer conditions in the late Pliocene than at present (e.g., Kou et al., 2006; Sun et al., 2011; Su et al., 2013). Mostly published as case studies, they demonstrate their capability to reveal the late Pliocene climatic regime at a given locality. However, the spatial variation of temperatures at that time which existed as a function of great geological and topographical complexity that characterized the region has not been studied. In addition, the patterns of summer and winter temperature changes since the late Pliocene have not been fully investigated.

In this study, we reconstruct quantitatively the palaeoclimates of eight late Pliocene floras from the SBTP that provide sufficient taxonomical information for the Coexistence Approach (CoA) proxy and are adequately dated. Palaeoclimates of three of the floras are reconstructed for the first time, and those of the remaining five floras are re-evaluated based on taxonomical data presented in previous studies. All the reconstructed palaeoclimates are compiled to achieve a clearer view of the late Pliocene temperature patterns of this region. They are compared with those of the present day to observe the temperature changes since the late Pliocene. The late Pliocene monsoon climate is also observed based on the reconstructed summer and winter precipitations.

2. Material and methods

2.1. Study area, fossil sites and ages

In this study, eight late Pliocene floras, including both mega- and microfossil assemblages, from the SBTP are compiled from published sources (Table 1 and Fig. 1). These floras contain at least 15 fossil taxa at the generic level, except for Lanping which contains only 10 fossil genera. The floras are well documented with regard to their stratigraphy and age (Table 1). Here, we use the age units based on the updated stratigraphic chart by Ogg (2012). The Miyi, Lanping and Eryuan floras belong to the Sanying Formation which is widely developed in the northwest of the SBTP region (WGYRGS, 1978; YBGMR, 1990). The Sanying Formation is dated as late Pliocene based on lithostratigraphy and biostratigraphy (Ge and Li, 1999), mammalian fossils (Su et al., 2011), and magnetostratigraphy (≈3.6 Ma, Li et al., 2013). The Yuanmou flora belongs to the Gantang Formation, which is determined as late Pliocene based on lithostratigraphic and biostratigraphic correlations (Liu et al., 2002; Yao et al., 2012). The Zhujie flora is referred to the Ciying Formation, which is constrained as late Pliocene based on lithostratigraphic correlations

Table 1
Eight late Pliocene floras in the SBTP, including information about location, geological age, dating method, fossil type and number of fossil taxa.

Flora	Location	Altitude (m)	Age	Formation	Time dating method	Fossil type	Number of Taxa (genera)	References
1. Miyi	102°01′E, 26°58′N	1150	Late Pliocene	Sanying	Lithostratigraphy, biostratigraphy	Leaf	28	Zhou (2000)
2. Lanping	99°26′E, 26°28′N	2740	Late Pliocene	Sanying	Lithostratigraphy, biostratigraphy, magnetostratigraphy	Leaf	10	Tao (1986) and Huang (2012)
3. Eryuan	99°49′E, 26°00′N	2100	Late Pliocene	Sanying	Lithostratigraphy, biostratigraphy, magnetostratigraphy	Pollen	21	Kou et al. (2006)
4. Yuanmou	101°48′E, 25°51′N	1030	Late Pliocene	Gantang	Lithostratigraphy, biostratigraphy	Leaf	21	Liu et al. (2002)
5. Zhujie	103°53′E, 25°11′N	2090	Late Pliocene	Ciying	Lithostratigraphy	Pollen	25	Wang and Shu (2004)
6. Yangyi	99°15′E, 24°57′N	1650	Late Pliocene	Yangyi	Lithostratigraphy, biostratigraphy	Pollen	19	Xu (2002)
7. Tuantian	98°38′E, 24°41′N	1250	Late Pliocene	Mangbang	Lithostratigraphy, biostratigraphy, isotopic dating	Leaf	19	Sun et al. (2011)
8. Longling	98°50′E, 24°41′N	1840	Late Pliocene	Yangyi	Lithostratigraphy, biostratigraphy	Pollen	25	Xu (2002) and Xu et al. (2004)

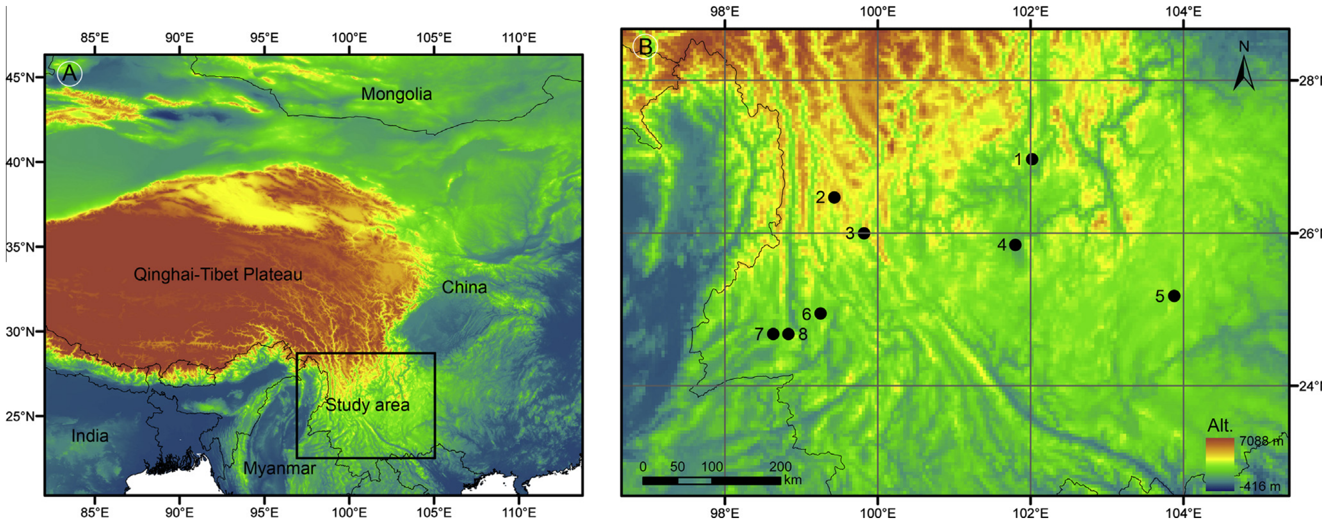

Fig. 1. Study area and localities of the eight late Pliocene floras. (A) Map showing the location of the study area; (B) map showing the localities of the eight late Pliocene floras in the SBTP region. The floral localities are numbered following Table 1.

(WGYRGS, 1978; YBGMR, 1990; Wang and Shu, 2004). The Yangyi and Longling floras belong to the Yangyi Formation, which is dated as late Pliocene based on lithostratigraphic and biostratigraphic comparisons (WGYRGS, 1978; YBGMR, 1990; Ge and Li, 1999; Xu et al., 2003). The Tuantian flora belongs to the Mangbang Formation, which is dated as late Pliocene based on lithostratigraphic and biostratigraphic correlations (WGYRGS, 1978; YBGMR, 1990; Ge and Li, 1999; Sun et al., 2011) as well as radiometric dating (3.297 ± 0.040 Ma, Li et al., 2000).

2.2. Palaeoclimatic reconstructions

Plant fossils are valuable proxies for quantitative palaeoclimatic reconstructions. As the eight floras in this study include both mega- and microfossils, we use the Coexistence Approach (CoA; Mosbrugger and Utescher, 1997) which functions with all types of plant organs provided their taxonomical statuses can be determined. This approach is based on the hypothesis that the fossil taxa have similar climatic requirements as those of their nearest living relatives (NLRs; Mosbrugger and Utescher, 1997). The climatic ranges in which a maximum numbers of NLRs of a given fossil flora can coexist are considered the general palaeoclimatic situation of the fossil flora (Utescher et al., 2014). To enable a maximum number of taxa to contribute to the CoA analysis, numerous climatic data sets of NLRs have been added to the database (Utescher and Mosbrugger, 2013) on which the present analysis was based. This updated database can be freely accessed at the Palaeoflora website (http://www.palaeoflora.de; Utescher and Mosbrugger, 2013).

For five of the eight late Pliocene floras, i.e., Eryuan, Yuanmou, Yangyi, Tuantian and Longling, palaeoclimates have already been quantitatively reconstructed using the CoA (Xu et al., 2003, 2004; Kou et al., 2006; Sun et al., 2011; Yao et al., 2012). The remaining three floras, i.e., Miyi, Lanping and Zhujie have not yet been studied with respect to palaeoclimate. To obtain a homogeneous data set, the five reconstructed floras were re-evaluated and the remaining three floras were calculated for the first time, both using the updated climatic database. Climatic requirements of the NLRs of the fossil taxa from the Miyi, Lanping and Zhujie flora are given in the Appendix (A, B, C). To minimize uncertainties related to taxonomic identification and assignment of the NLRs, the coexistence intervals are calculated based on the climatic requirements of the NLRs at the generic level. Six palaeoclimatic parameters are calculated, including mean annual temperature (MAT), mean temperature of the warmest month (WMMT), mean temperature of the coldest month (CMMT), mean annual precipitation (MAP), mean precipitation of the wettest month (MP WET), and mean precipitation of the driest month (MP DRY).

2.3. Spatial analysis

Means of the palaeoclimatic parameters are calculated using the minimum and maximum values of the reconstructed CoA intervals for each climatic parameter considered. Anomalies are calculated as the differences between the calculated palaeoclimatic parameters and modern values. Means of the anomalies are calculated using the minimum and maximum values of the calculated anomaly intervals. Modern climatic information at the fossil sites is obtained from their nearest meteorological stations (Yunnan Meteorological Bureau, 1984). The climates recorded at the meteorological stations can be used as modern climates at the fossil sites, because the fossil sites have comparable altitudes with their nearest meteorological stations. The reconstructed temperatures, and temperature and precipitation anomalies are displayed using spatial analysis tools of the geographical information software ArcGis 9.3 (Esri Company, Redlands). The comparative spatial temperature variations for the present-day are based on the basic worldwide climatic data (Hijmans et al., 2005). They are also displayed using spatial analysis tools of the geographical information software ArcGis 9.3.

3. Results

The calculated and re-evaluated palaeoclimatic parameters, together with their means, of the eight late Pliocene floras are given in Table 2. Temperatures including MATs, WMMTs and CMMTs are displayed in Fig. 2 to visualize spatial gradients during the late Pliocene. As is shown, temperatures in the northern part of the SBTP were clearly lower while those in its southern part were higher. The northwestern part appears to have the lowest temperatures (Fig. 2). The three temperature-related parameters are further displayed in Fig. 3 to show their comparisons with modern values. The late Pliocene temperatures seem higher than today, but those in a few places such as Yuanmou were even lower than the present-day (Fig. 3).

Anomalies of five climatic parameters, i.e., MAT, WMMT, CMMT, MP WET and MP DRY and their means are given in Table 3. Anomalies of the WMMTs and CMMTs are further illustrated in Fig. 4 to visualize the changes of summer and winter temperatures,

Table 2
The reconstructed six climatic parameters for the eight late Pliocene floras in the SBTP. Climatic parameters for five floras, i.e., Eryuan, Yuanmou, Yangyi, Tuantian and Longling are re-evaluated based on palaeobotanical information given by Kou et al. (2006), Yao et al. (2012), Xu et al. (2003, 2004), Sun et al. (2011) and Xu et al. (2004), respectively, using the extended and updated NLR climatic database. Climatic parameters for the remaining three floras, i.e., Miyi, Lanping and Zhujie are presented for the first time.

Site	Age	MAT (°C)	Mean (°C)	WMMT (°C)	Mean (°C)	CMMT (°C)	Mean (°C)	MAP (mm)	Mean (mm)	MP WET (mm)	Mean (mm)	MP DRY (mm)	Mean (mm)	Palaeoclimatic data
1. Miyi	Late Pliocene	15.5–18.6	17.05	25.4–28.1	26.75	3.1–8.1	5.6	1019–1335	1177	182–225	203.5	9–58	33.5	This study
	Modern	16.7		22.1		9.1		1060		219		6		
2. Lanping	Late Pliocene	7–17.4	12.2	16.9–27	21.95	-3.1–8.3	2.6	552–1151	851.5	116–149	132.5	5–57	31	This study
	Modern	11.3		17.9		3.4		1025		215		8		
3. Eryuan	Late Pliocene	11.5–17.5	14.5	23–27.9	25.45	-1–7.7	3.5	620–1483	1051.5	109–139	124	9–55	32	Kou et al. (2006), re-evaluated
	Modern	12.8		18.2		6.2		1048		187		19		
4. Yuanmou	Late Pliocene	14.8–17.4	16.1	19.8–27.6	23.7	2–6	4	1484–1784	1634	166–183	174.5	13–25	19	Yao et al. (2012), re-evaluated
	Modern	21.8		27		14.5		634		141		3		
5. Zhujie	Late Pliocene	15.7–18.4	17.05	23–28.1	25.55	9.6–12.5	11.05	892–982	937	109–178	143.5	18–41	29.5	This study
	Modern	14.4		19.9		6.9		1058		232		14		
6. Yangyi	Late Pliocene	11.6–18.4	15	23–28.2	25.6	-0.3–12.5	6.1	798–1255	1026.5	116–293	204.5	16–41	28.5	Xu (2002), re-evaluated
	Modern	15.6		20.9		8.1		974		188		13		
7. Tuantian	Late Pliocene	15.6–20.8	18.2	26.5–28.1	27.3	6–13.3	9.65	1377–1695	1536	204–248	226	19–55	37	Sun et al. (2011), re-evaluated
	Modern	14.9		19.8		7.6		1452		271		19		
8. Longling	Late Pliocene	17.5–20.8	19.15	24–28.1	26.05	9.6–13.3	11.45	816–1255	1035.5	225–293	259	9–55	32	Xu et al. (2004), re-evaluated
	Modern	15		19.9		7.4		2084		475		15		

respectively, since the late Pliocene. The WMMTs were generally higher than those at present, except for that of Yuanmou (Fig. 4). The CMMTs appear generally similar to the modern values. Those of only a few sites have changed, e.g., the CMMT of Zhujie has declined while that of Yuanmou has increased since the late Pliocene. Anomalies of the MP WETs and MP DRYs are illustrated in Fig. 5 to visualize the changes of summer and winter precipitations, respectively. It is evident that the MP WETs have generally increased whereas the MP DRYs have significantly decreased.

4. Discussion

4.1. Spatial temperature gradients

As is shown in Table 2 and Fig. 2, Lanping and Eryuan as the most northwesterly of the eight sites have lower MAT estimates, with values being 7–17.4 °C and 11.5–17.5 °C, respectively. Zhujie, Tuantian and Longling as the most southerly of the eight sites yield higher MAT estimates, with values being 15.7–18.4 °C, 15.6–20.8 °C and 17.5–20.8 °C, respectively. The remaining three sites have intermediate MAT estimates. This suggests spatial temperature gradients in the SBTP during the late Pliocene: the northwest was cooler while the south was warmer. This pattern of temperature gradients can also be seen in the WMMT and CMMT (Table 2 and Fig. 2).

Usually, surface temperature gradients are mainly correlated to differences in altitude or latitude or both. Although there is so far no evidence from the SBTP, we expect the latitudinal temperature gradient to be generally similar to the value in other regions of the Northern Hemisphere, e.g., Europe, which was estimated to have been 0.6–0.65 °C per degree in the Pliocene (Fauquette et al., 2007). Hence the mean annual temperature difference between the northern most site namely Lanping and the three southern most sites namely Zhujie, Tuantian and Longling would be approximately 1.2 °C. In fact, the late Pliocene MAT at Lanping was 1–8.7 °C, 3.4–8.6 °C and 3.4–8.5 °C lower than that at Zhujie, Tuantian and Longling, respectively. These spatial differences in MAT are much larger than expected. We therefore tend to believe that the steep temperature gradients observed were largely attributable to altitudinal differences while latitude played only a subordinate role. Because of the southeastward extrusion of the Qinghai–Tibet Plateau and intense mountain uplift, altitude increased in the SBTP during the late Cenozoic (Schoenbohm et al., 2004, 2006; Shen et al., 2005). The late Pliocene temperature gradients suggest that the northern part might have increased more significantly than the southern part of this region. In addition, the northwestern part probably constituted the area with the greatest altitude during that time. This is in line with previous understandings that the southern part of the SBTP uplifted later, primarily during the Pliocene and Quaternary (Schoenbohm et al., 2004, 2006).

Today, the SBTP region is famous for its topographical diversity and complexity, with altitude varying enormously from 6750 m in the northwest to only around 500 m in the south (Wang and Zhang, 2002; Wang, 2006). Correspondingly, the climatic regime varies from the cold alpine meadows in the northwest to warm seasonal rain forests in the south (Yunnan Meteorological Bureau, 1984; Wang and Zhang, 2002; Wang, 2006). Our results would seem to suggest that this pattern of temperature gradients related to altitude became established by the late Pliocene.

4.2. Mean annual temperature changes

The late Pliocene is widely recognized as having warmer conditions than today, both globally and regionally (Haywood et al.,

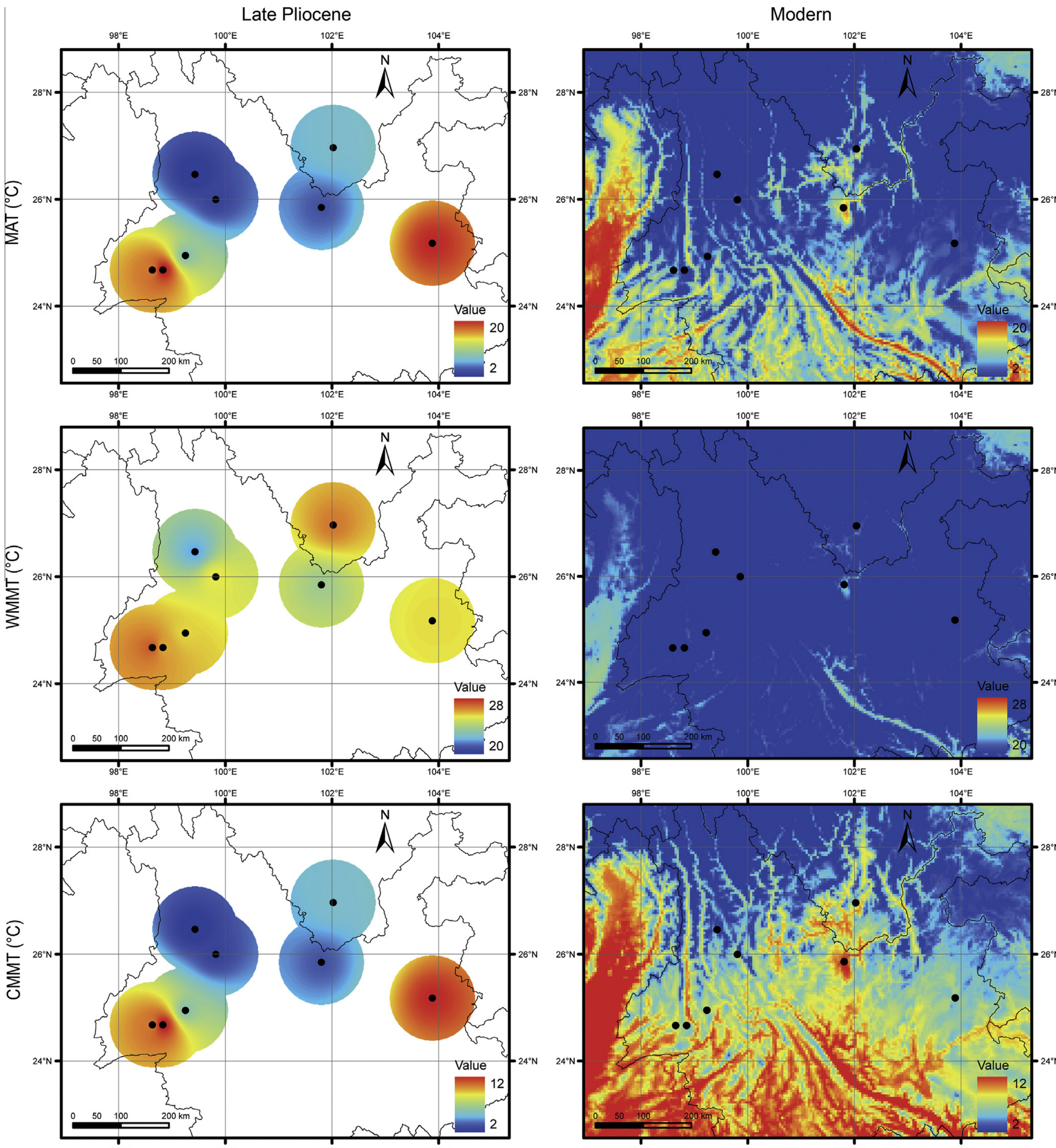

Fig. 2. Spatial temperature gradients in the late Pliocene and at present in the study area.

2000; Haywood and Valdes, 2004; Mosbrugger et al., 2005; Uhl et al., 2007; Dowsett et al., 2009; Lunt et al., 2010; Brigham-Grette et al., 2013). In the SBTP, MAT estimates from the eight sites except Yuanmou are generally higher than those at present (Table 2). This is also demonstrated by the calculated MAT anomalies and their means (Table 3). Yuanmou was exceptional in having a much lower MAT in the late Pliocene (Fig. 3). Today's higher temperatures at Yuanmou are thought to be attributed to a Foehn wind effect and the development of warm dry valleys (Yao et al., 2012). This suggests that the warm dry deep valleys now existing at Yuanmou were probably not yet established in the late Pliocene. Based on the above comparisons in MAT, it is evident that the late Pliocene SBTP was overall warmer than at present though Yuanmou was exceptionally cooler, in agreement with previous palaeoclimatic investigations in this region (Xu, 2002; Xu et al., 2004; Kou et al., 2006; Sun et al., 2011; Xie et al., 2012; Su et al., 2013).

As suggested by various studies, mean global temperature declined around 2–3 °C since the late Pliocene (Haywood et al., 2000; Lunt et al., 2010; Salzmann et al., 2011). However, the cooling trend did not affect all regions to the same degree. In the Northern Hemisphere, it is thought to be most pronounced

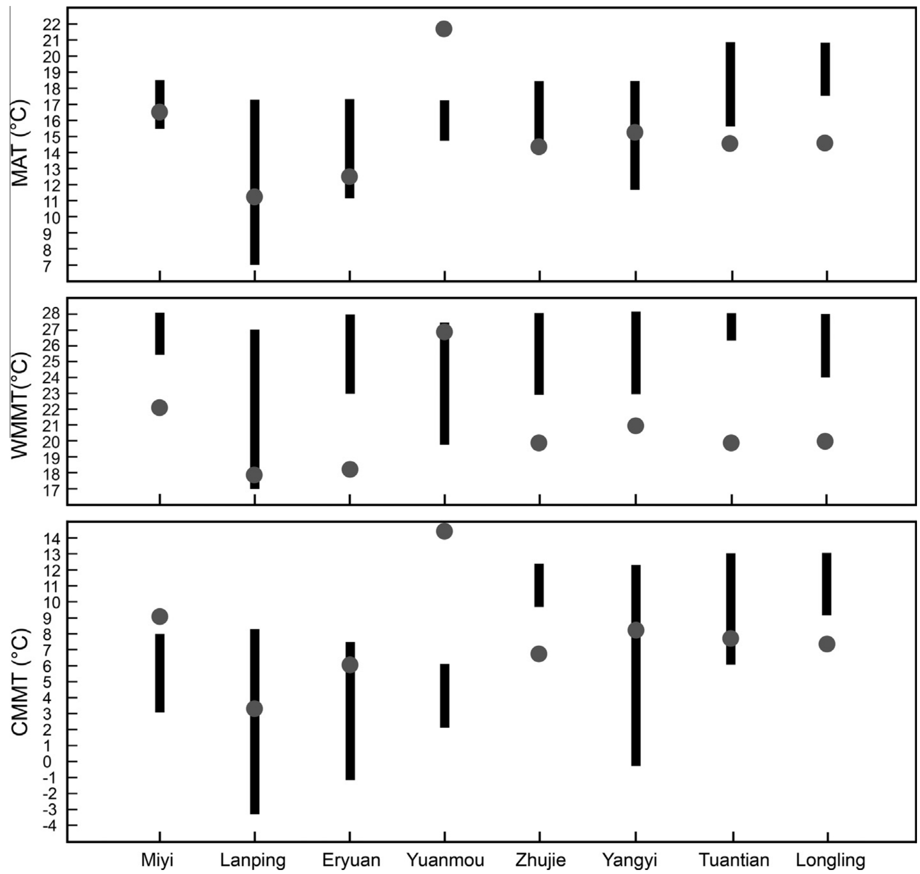

Fig. 3. Chart showing the intervals of the reconstructed late Pliocene MATs, CMMTs and WMMTs (bars) in the study area, and their comparisons with modern values (dots).

Table 3
Late Pliocene anomaly ranges and their mean values for five climatic parameters.

Site	MAT anomaly (°C)	Mean (°C)	WMMT anomaly (°C)	Mean (°C)	CMMT anomaly (°C)	Mean (°C)	MP WET anomaly (mm)	Mean (mm)	MP DRY anomaly (mm)	Mean (mm)
1. Miyi	−1.2–1.9	0.35	3.3–6	4.65	−6–(−1)	−3.5	−37–6	−15.5	3–52	27.5
2. Lanping	−4.3–6.1	0.9	−1–9.1	4.05	−6.5–4.9	−0.8	−99–(−66)	−82.5	−3–49	23
3. Eryuan	−1.3–4.7	1.7	4.8–10	7.4	−7.2–1.5	−2.85	−78–(−48)	−63	−10–36	13
4. Yuanmou	−7–(−4.4)	−5.7	−7.2–0.6	−3.3	−12.5–(−8.5)	−10.5	25–42	33.5	10–22	16
5. Zhujie	1.3–4	2.65	3.1–8.3	5.7	2.7–5.6	4.15	−123–(−54)	−88.5	4–37	20.5
6. Yangyi	−4–2.8	−0.6	2.1–7.3	4.7	−8.3–4.4	−1.95	−72–105	16.5	3–28	15.5
7. Tuantian	0.7–5.9	3.3	6.7–8.3	7.5	−1.6–5.7	2.05	−68–(−24)	−46	0–36	18
8. Longling	2.5–5.8	4.15	4.1–8.2	6.15	2.2–5.9	4.05	−250–(−182)	−216	−6–40	18

in mid to high latitudes (Mosbrugger et al., 2005; Uhl et al., 2007; Utescher et al., 2011). For example, Central Europe experienced a MAT decline of around 5 °C since the late Pliocene, based on evidence from palaeobotanical proxy data (Mosbrugger et al., 2005). The late Pliocene temperatures from relatively low latitudes have not been extensively studied so far, except for palaeoclimatic model simulations (e.g., Haywood et al., 2000; Haywood and Valdes, 2004). The present study area, ranging from 24.5° to 27° N (Fig. 1, B), does not strictly represent a low latitude region, but clearly has a more southerly position than Central Europe. As discussed above, most studied sites in the SBTP indicate a temperature decline since the late Pliocene. MAT anomalies, ranging from −0.6 °C to 4.15 °C, suggest a mean temperature decline of about 1 °C since the late Pliocene, far lower than 5 °C of temperature decline in Central Europe. This is consistent with previous interpretations that the post-Pliocene cooling was more pronounced in the northern higher latitudes than in the lower ones (Uhl et al., 2007; Utescher et al., 2011).

4.3. Decline of summer and winter temperatures

The WMMTs estimated from the eight fossil sites except for Yuanmou are generally higher than their modern values, suggesting warmer summers in the late Pliocene (Figs. 3 and 4). In contrast to the WMMTs, the CMMTs estimated from the eight sites approximate the present-day figures: Miyi and Yuanmou had higher CMMTs, Zhujie and Longling had slightly lower CMMTs than today, while the remaining four sites had CMMTs comparable to the present (Figs. 3 and 4). All these indicate that in the SBTP, the WMMT has declined significantly while the CMMT has not changed notably since the late Pliocene. In other words, summer temperature has declined markedly while winter temperature has changed only moderately, in agreement with a recent palaeoclimatic observation from the western part of this region (Su et al., 2013).

It is believed that the Cenozoic global surface cooling is more pronounced for the CMMT than the WMMT and MAT (Utescher et al., 2000; Mosbrugger et al., 2005). In the present study area, however, the WMMT rather than the CMMT displays the most

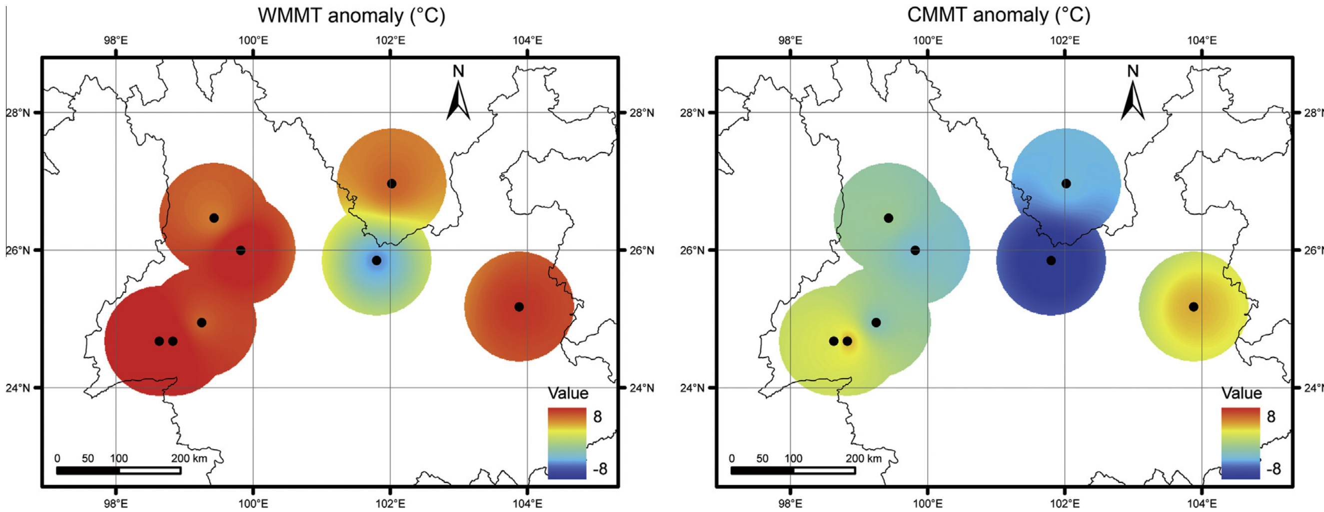

Fig. 4. WMMT and CMMT anomalies at a mean of the eight late Pliocene floras in the study area.

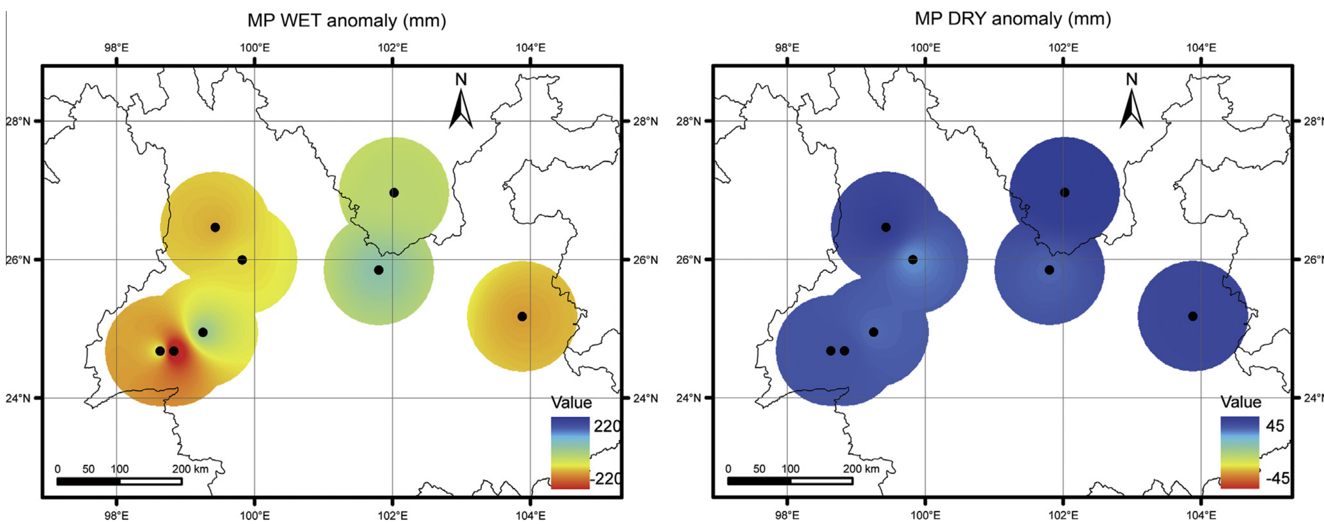

Fig. 5. MP WET and MP DRY anomalies at a mean of the eight late Pliocene floras in the study area.

pointed declining trend. This unexpected pattern is probably attributable to the eastward extrusion of the Qinghai–Tibet Plateau and related processes of tectonic uplift that has impacted regional atmospheric circulation patterns. In monsoonal zones of East Asia, winter temperatures are usually related to the intensity of the Asian winter monsoon. In the cold season, a high pressure system originates over the Siberian-Mongolian region and causes the southward flow of cold air masses, thus bringing down winter temperatures across monsoon-affected areas of East Asia (Ding, 1994; Wu and Chan, 1997; Chang et al., 2006). The post-Pliocene eastern extrusion of the Qinghai–Tibet Plateau created high mountainous areas to the north of the study area (England and Houseman, 1989; Williams et al., 2001; Zhang and Ding, 2003; Zhang et al., 2006; Xu et al., 2008). The extended eastern Qinghai–Tibet Plateau, having an average altitude of over 3000 m, possibly blocked the intrusion of cold surges from the north, and forced them to circumvent the eastern flank of the plateau (Chang et al., 2006; Molnar et al., 2010; Chang and Lu, 2012). This process would have weakened the impact of the cold winter monsoon on the study area, and thus would explain the relatively high present level of winter temperatures with respect to late Pliocene values. On the other hand, the study area itself experienced overall intense mountain uplift since the late Pliocene (Schoenbohm et al., 2004, 2006; Shen et al., 2005). The increase in altitude should have led to a decline of both summer and winter temperatures. The balance between the related warming caused by the eastern extrusion of the Qinghai–Tibet Plateau, and the cooling caused by mountain uplift and the global surface cooling probably resulted in the insignificant winter cooling. Meanwhile, the post late Pliocene mountain uplift plus the global signal might have resulted in the pronounced summer cooling.

4.4. Weaker monsoon climate

Located in East Asia, the SBTP has had higher precipitation in summer and lower precipitation in winter, a characteristic of the Asian monsoon climate, at least since the early Miocene (Sun and Wang, 2005; Guo et al., 2008). We therefore assume that the MP WET and MP DRY in this region can roughly represent the precipitations of summer and winter, respectively. As is shown (Table 2 and Fig. 5), estimates of the MP WETs from the eight fossil sites are generally lower while estimates of the MP DRYs are overall higher than their modern values. This indicates a weaker monsoon climate in the SBTP during the late Pliocene. The increased summer rainfall and decreased winter one suggest an intensification of the monsoon since the late Pliocene, which was probably related to mountain uplift in the west of this region (Su et al., 2013).

5. Conclusions

Impacted by the uplift and expansion of the Qinghai–Tibet Plateau, the SBTP has experienced drastic topographic and climatic changes since the late Pliocene. Quantitative palaeoclimatic reconstructions performed on eight late Pliocene floras from this region lead to the following conclusions:

(1) Spatial temperature gradients occurred in the SBTP during the late Pliocene: the northwest was cooler while the south was considerably warmer than other parts of the region. This pattern of temperature gradients is largely attributed to differences in altitude: the northwest was already higher than the south of the SBTP at that time.
(2) Compared to the marked global cooling since the late Pliocene, the temperature decline in the SBTP is only minor. The cooling trend in this region is not as pronounced as that observed from the mid to high latitudes in Central Europe. This is consistent with previous interpretations that the late Cenozoic cooling is most pronounced in the northern mid to high latitudes, but minimal in lower latitude regions.
(3) The post late Pliocene summer cooling is pronounced while winter temperatures have remained more or less unchanged since the late Pliocene. This is at variance with previous observations from other territories. This unexpected pattern of cooling trend can be attributed to the eastward extrusion of the Qinghai–Tibet Plateau and mountain uplift since the late Pliocene. The eastward extrusion of the plateau probably weakened the impact of the cold high pressure on this region in winter. The post-Pliocene mountain uplift in the whole region caused the decline of both summer and winter temperatures.
(4) Summer precipitation increased while winter precipitation decreased since the late Pliocene, suggesting an intensification of the Asia monsoon climate in this region.

Acknowledgements

This work is supported by the National Natural Science Foundation of China, NNSFC (Nos. 31300187 and 41030212), the National Basic Research Program of China, 973 Program (No. 2012CB821900), U.S. DOE DE-AC02-06CH11357, and the Foundation of the State Key Laboratory of Palaeobiology and Stratigraphy, Nanjing Institute of Geology and Palaeontology, Chinese Academy of Sciences (No. 123107). Torsten Utescher thanks the German Science Foundation for financial support. This work is a contribution to NECLIME (Neogene Climate of Eurasia).

Appendix A. Fossil taxa at the generic level and climatic requirements of their NLRs of three late Pliocene floras in the SEBQTP.

A. Fossil taxa at the generic level and climatic requirements of their NLRs of the late Pliocene Miyi flora (palaeobotanical data based on Zhou, 2000).

Fossil taxa at generic level	NLRs	MAT (°C)		CMMT (°C)		WMMT (°C)		MAP (mm)		MP WET (mm)		MP DRY (mm)	
		Min	Max	Min	Max	Min	Max	Min	Max	Min	Max	Min	Max
Acer sp.	*Acer* sp.	−0.4	24	−24.2	20.6	12.9	29.3	115	2559	19	370	1	135
Albizzia sp.	*Albizzia* sp.	14.8	28	2.5	27	19.8	32.5	307	3151	81	558	0	165
Betula sp.	*Betula* sp.	−15	25.8	−41	21.1	1.3	28.7	110	2559	23	353	0	135
Camellia sp.	*Camellia* sp.	13.8	27.7	1.8	27	25.4	29.6	1090	3151	182	605	2	165
Castanopsis sp.	*Castanopsis* sp.	9.3	27.9	−1.5	27	12.7	32.5	397	3151	68	610	0	165
Cinnamomum sp.	*Cinnamomum* sp.	13.5	27.2	2.5	26.1	18.6	31.7	828	3293	160	988	3	135
Corylopsis sp.	*Corylopsis* sp.	9.1	18.6	−2.7	8.1	22.3	28.8	979	1562	148	304	7	67
Cyclocarya sp.	*Cyclocarya* sp.												
Desmodium sp.	*Desmodium* sp.												
Engelhardia sp.	*Engelhardia* sp.	13.8	27	3.1	25	22.1	33.6	823	3172	204	518	5	152
Eurya sp.	*Eurya* sp.	9.1	27.7	−2.9	27	15.9	31.1	1065	3151	116	422	1	165
Fraxinus sp.	*Fraxinus* sp.	0	24	−25.8	16.7	14.9	33.9	148	1844	28	358	2	95
Gordonia sp.	*Gordonia* sp.	14.4	25.5	0.9	21.4	20.2	29.2	810	2100	106	304	3	74
Ilex sp.	*Ilex* sp.	−0.4	27.7	−12.9	27	10.4	33.6	641	3151	98	389	2	165
Indigofera sp.	*Indigofera* sp.	15.5	27.7	2.2	26.1	20.2	29.2	815	3370	60	479	9	165
Juglans sp.	*Juglans* sp.	0	27.5	−22.7	25	9.5	31.2	210	2617	28	582	1	114
Laurifolia sp.	*Laurifolia* sp.												
Lespedeza sp.	*Lespedeza* sp.												
Lindera sp.	*Lindera* sp.	9.3	27.7	−7.3	27	21.6	28.1	396	3151	90	389	4	165
Lithocarpus sp.	*Lithocarpus* sp.	7	27.1	−3.1	23.5	16.7	29.9	529	2395	116	379	0	64
Litsea sp.	*Litsea* sp.	13.6	27.7	2.2	27	20.9	28.6	816	3151	109	389	7	165
Myrica sp.	*Myrica* sp.	−8.9	28.1	−29	27	8.9	33.9	233	3151	34	508	0	165
Populus sp.	*Populus* sp.	−16	26	−49	13.6	9.8	35.6	25	2559	8	358	0	93
Quercus sp.	*Quercus* sp.	−1.4	27	−25.1	25.9	8.4	28.3	201	3905	33	610	0	180
Rhododendron sp.	*Rhododendron* sp.	−12	27.7	−27.9	27	3.9	28.1	110	3151	23	389	3	165
Smilax sp.	*Smilax* sp.	−1.1	27.7	−25.8	27	15.1	33.1	37	3151	8	389	0	165
Thermopsis sp.	*Thermopsis* sp.	−3.2	22.8	−25.6	13.6	13.5	28.5	201	1335	33	225	0	58
Ulmus sp.	*Ulmus* sp.	−4.9	26.6	−25.8	26.1	16	29.4	201	3285	33	569	0	75

B. Fossil taxa at the generic level and climatic requirements of their NLRs of the late Pliocene Lanping flora (palaeobotanical data based on Tao, 1986; Huang, 2012).

Fossil taxa at generic level	NLRs	MAT (°C)		CMMT (°C)		WMMT (°C)		MAP (mm)		MP WET (mm)		MP DRY (mm)	
		Min	Max	Min	Max	Min	Max	Min	Max	Min	Max	Min	Max
Acer sp.	*Acer* sp.	−0.4	24	−24.2	20.6	12.9	29.3	115	2559	19	370	1	135
Berberis sp.	*Berberis* sp.	−4.9	18	−32.4	10	15	27.1	304	2336	45	454	0	75
Desmodium sp.	*Desmodium* sp.												
Hippophae sp.	*Hippophae* sp.	1.6	17.4	−11.1	8.3	13.4	27	552	1151	64	149	5	57
Lithocarpus sp.	*Lithocarpus* sp.	7	27.1	−3.1	23.5	16.7	29.9	529	2395	116	379	0	64
Picea sp.	*Picea* sp.	−8.9	21.7	−28.6	15.6	7.3	31.6	142	6000	36	700	2	400
Pinus sp.	*Pinus* sp.	−9.2	25.5	−36.8	21.4	7.1	32.9	180	1741	28	293	0	94
Populus sp.	*Populus* sp.	−16	26	−49	13.6	9.8	35.6	25	2559	8	358	0	93
Quercus sp.	*Quercus* sp.	−1.4	27	−25.1	25.9	8.4	28.3	201	3905	33	610	0	180
Salix sp.	*Salix* sp.	−17	27.7	−50.1	26.5	7.6	32.9	122	2399	22	448	0	108

C. Fossil taxa at the generic level and climatic requirements of their NLRs of the late Pliocene Zhujie flora (palaeobotanical data based on Wang and Shu, 2004).

Fossil taxa at generic level	NLRs	MAT (°C)		CMMT (°C)		WMMT (°C)		MAP (mm)		MP WET (mm)		MP DRY (mm)	
		Min	Max	Min	Max	Min	Max	Min	Max	Min	Max	Min	Max
Abies sp.	*Abies* sp.	−6.7	27.4	−26	25.6	7.1	29.5	373	2648	57	369	0	135
Alnus sp.	*Alnus* sp.	−13.3	27.4	−40.9	25.6	12	38.6	41	2559	8	353	0	135
Artemisia sp.	*Artemisia* sp.												
Carya sp.	*Carya* sp.	4.4	26.6	−11.5	22.2	19.3	30.6	373	1724	68	434	8	93
Castanea sp.	*Castanea* sp.	8.7	24.2	−3.9	16.7	21.6	29.4	473	1857	70	424	3	88
Cedrus sp.	*Cedrus* sp.	11.6	18.4	−0.3	12.5	19.4	31.8	164	1577	43	434	0	41
Celtis sp.	*Celtis* sp.	2.5	25.8	−17.7	23	18.7	28.8	116	2730	25	597	0	88
Elaeagnus sp.	*Elaeagnus* sp.	−0.4	27.7	−24.2	27	18.2	28.5	84	3151	28	389	2	165
Ephedra sp.	*Ephedra* sp.	3.1	28.8	−12	25	16.4	32.9	33	932	5	178	0	45
Euphorbia sp.	*Euphorbia* sp.												
Fagus sp.	*Fagus* sp.	4.4	23.1	−11.5	17	17.3	28.5	376	2648	46	448	5	94
Ilex sp.	*Ilex* sp.	−0.4	27.7	−12.9	27	10.4	33.6	641	3151	98	389	2	165
Juglans sp.	*Juglans* sp.	0	27.5	−22.7	25	9.5	31.2	210	2617	28	582	1	114
Liquidambar sp.	*Liquidambar* sp.	11.5	24.6	−1	23.8	23	29.3	619	1823	109	340	2	72
Lycopodium sp.	*Lycopodium* sp.												
Microlepia sp.	*Microlepia* sp.	15.7	27.7	9.6	27	20.2	28.5	892	3151	208	398	3	165
Osmunda sp.	*Osmunda* sp.	0.2	25.8	−16.6	24.1	16.3	29.5	206	4150	34	914	2	59
Picea sp.	*Picea* sp.	−8.9	21.7	−28.6	15.6	7.3	31.6	142	6000	36	700	2	400
Pinus sp.	*Pinus* sp.	−9.2	25.5	−36.8	21.4	7.1	32.9	180	1741	28	293	0	94
Polygonum sp.	*Polygonum* sp.	−0.6	21.7	−12.8	14.8	15.6	28.2	435	2559	63	454	1	135
Quercus sp.	*Quercus* sp.	−1.4	27	−25.1	25.9	8.4	28.3	201	3905	33	610	0	180
Rhus sp.	*Rhus* sp.	3.4	24.9	−12.9	22.2	18.9	29.4	735	1613	73	389	18	93
Salix sp.	*Salix* sp.	−17	27.7	−50.1	26.5	7.6	32.9	122	2399	22	448	0	108
Tilia sp.	*Tilia* sp.	2.5	20.8	−17.7	13.3	15	28.1	373	1958	68	454	9	83
Tsuga sp.	*Tsuga* sp.	−1.8	21.9	−15.6	15.6	11	29.5	285	2648	48	350	0	108

References

Biasatti, D., Wang, Y., Deng, T., 2010. Strengthening of the East Asian summer monsoon revealed by a shift in seasonal patterns in diet and climate after 2–3 Ma in northwest China. Palaeogeogr. Palaeoclimatol. Palaeoecol. 297, 12–25.

Brigham-Grette, J., Melles, M., Minyuk, P., Andreev, A., Tarasov, P., DeConto, R., Koenig, S., Nowaczyk, N., Wennrich, V., Rosén, P., Haltia, E., Cook, T., Gebhardt, C., Meyer-Jacob, C., Snyder, J., Herzschuh, U., 2013. Pliocene warmth, polar amplification, and stepped Pleistocene cooling recorded in NE Arctic Russia. Science 340, 1420–1427.

Chang, C.-P., Lu, M.-M., 2012. Intraseasonal predictability of Siberian high and east Asian winter monsoon and its interdecadal variability. J. Clim. 25, 1773–1778.

Chang, C.-P., Wang, Z., Hendon, H., 2006. The Asian winter monsoon. In: Wang, B. (Ed.), The Asian Monsoon. Praxis, Springer, Berlin-Heidelberg, pp. 89–127.

Clark, M.K., Royden, L.H., 2000. Topographic ooze: building the eastern margin of Tibet by lower crustal flow. Geology 28, 703–706.

Ding, Y., 1994. Monsoons over China. Kluwer Academic Publishers, Dordrecht, The Netherlands, 510 pp.

Dowsett, H.J., Robinson, M.M., Foley, K.M., 2009. Pliocene three-dimensional global ocean temperature reconstruction. Clim. Past 5, 769–783.

England, P., Houseman, G., 1989. Extension during continental convergence, with application to the Tibetan Plateau. J. Geophys. Res. 94, 17561–17579.

Fauquette, S., Suc, J.-P., Jiménez-Moreno, G., Micheels A., Jost, A., Favre, E., Bachiri-Taoufiq, N., Bertini, A., Clet-Pellerin, M., Diniz, F., Farjanel, G., Feddi, N., Zheng, Z., 2007. Latitudinal climatic gradients in the Western European and Mediterranean regions from the Mid-Miocene (c. 15 Ma) to the Mid-Pliocene (c. 3.5 Ma) as quantified from pollen data. In: Williams, M., Haywood, A.M., Gregory, F.J., Schmidt, D.N. (Eds.), Deep-Time Perspectives On Climate Change:

Marrying the Signal from Computer Models and Biological Proxies. The Micropalaeontological Society, Special Publications. The Geological Society, London, pp. 481–502.
Ge, H.-R., Li, D.-Y., 1999. Cenozoic Coal-bearing Basins and Coal-forming Regularity in West Yunnan. Yunnan Science and Technology Press, Kunming, 132 pp (in Chinese).
Guo, Z.-T., Sun, B., Zhang, Z.-S., Peng, S.-Z., Xiao, G.-Q., Ge, J.-Y., Hao, Q.-Z., Qiao, Y.-S., Liang, M.-Y., Liu, J.-F., Yin, Q.-Z., Wei, J.-J., 2008. A major reorganization of Asian climate by the early Miocene. Clim. Past 4, 153–174.
Harris, N., 2006. The elevation history of the Tibetan Plateau and its implications for the Asian monsoon. Palaeogeogr. Palaeoclimatol. Palaeoecol. 241, 4–15.
Haywood, A.M., Valdes, P.J., 2004. Modeling Pliocene warmth: contribution of atmosphere, oceans and cryosphere. Earth Planet. Sci. Lett. 218, 363–377.
Haywood, A.M., Valdes, P.J., Sellwood, B.W., 2000. Global scale palaeoclimate reconstruction of the middle Pliocene climate using the UKMO GCM: initial results. Global Planet. Change 25, 239–256.
Hijmans, R.J., Cameron, S.E., Parra, J.L., Jones, P.G., Jarvis, A., 2005. Very high resolution interpolated climate surface for global land areas. Int. J. Climatol. 25, 1965–1978.
Huang, Y.-J., 2012. The late Pliocene Fudong Flora from Lanping, Yunnan, and the Neogene climates in Hengduan Mountains. Ph.D. Thesis, Kunming Institute of Botany, Chinese Academy of Sciences, Kunming, China (in Chinese with English abstract).
Kou, X.-Y., Ferguson, D.K., Xu, J.-X., Wang, Y.-F., Li, C.-S., 2006. The reconstruction of palaeovegetation and palaeoclimate in the Late Pliocene of west Yunnan, China. Clim. Change 77, 431–448.
Kutzbach, J.E., Prell, W.L., Ruddiman, W.F., 1993. Sensitivity of Eurasian climate to surface uplift of the Tibetan Plateau. J. Geol. 101, 177–190.
Li, D.-M., Li, Q., Chen, W.-J., 2000. Volcanic activities in the Tengchong volcano area since Pliocene. Acta Petrologica Sinica 16, 362–370 (in Chinese with English abstract).
Li, S., Deng, C., Yao, H., Huang, S., Liu, C., 2013. Magnetostratigraphy of the Dali Basin in Yunnan and implications for late Neogene rotation of the southeast margin of the Tibetan Plateau. J. Geophys. Res.: Solid Earth 118, 791–807.
Liu, G.-W., Li, D.-Y., Huang, F., Fu, Q.-L., 2002. A Pliocene flora from the Gangtang Formation of Yuanmou Basin, Yunnan Province, SW China and its palaeoclimate significance. Acta Palaeontologica Sinica 41, 1–9 (in Chinese with English abstract).
Lunt, D.J., Haywood, A.M., Schmidt, G.A., Salzmann, U., Valdes, P.J., Dowsett, H.J., 2010. Earth system sensitivity inferred from Pliocene modeling and data. Nat. Geosci. 3, 60–64.
Molnar, P., Boos, W.R., Battisti, D.S., 2010. Orographic controls on climate and palaeoclimate of Asia: thermal and mechanical roles for the Tibetan Plateau. Annu. Rev. Earth Planet. Sci. 38, 77–102.
Mosbrugger, V., Utescher, T., 1997. The coexistence approach—a method for quantitative reconstructions of Tertiary terrestrial palaeoclimate data using plant fossils. Palaeogeogr. Palaeoclimatol. Palaeoecol. 134, 61–86.
Mosbrugger, V., Utescher, T., Dilcher, D.L., 2005. Cenozoic continental climatic evolution of Central Europe. PNAS 102, 14964–14969.
Ogg, G., 2012. Phanerozoic and Precambrian Chronostratigraphy. <http://www.stratigraphy.org>.
Salzmann, U., Williams, M., Haywood, A.M., Johnson, A.L.A., 2011. Climate and environment of a Pliocene warm world. Palaeogeogr. Palaeoclimatol. Palaeoecol. 309, 1–8.
Schoenbohm, L.M., Whipple, K.X., Burchfiel, B.C., Chen, L.-Z., 2004. Geomorphic constraints on surface uplift, exhumation, and plateau growth in the Red River region, Yunnan Province, China. Geol. Soc. Am. Bull. 116, 895–909.
Schoenbohm, L.M., Burchfiel, B.C., Chen, L.-Z., 2006. Propagation of surface uplift, lower crustal flow, and Cenozoic tectonics of the southeast margin of the Tibetan Plateau. Geology 34, 813–816.
Shen, Z.-K., Lü, J., Wang, M., Bürgmann, R., 2005. Contemporary crustal deformation around the southeast borderland of the Tibetan Plateau. J. Geophys. Res. 110, B11409.
Su, T., Jacques, F.M.B., Liu, Y.S., Xiang, J.Y., Xing, Y.W., Huang, Y.J., Zhou, Z.K., 2011. A new *Drynaria* (Polypodiaceae) from the upper Pliocene of Southwest China. Rev. Palaeobot. Palynol. 164, 132–142.
Su, T., Jacques, F.M.B., Spicer, R.A., Liu, Y.-S., Huang, Y.-J., Xing, Y.-W., Zhou, Z.-K., 2013. Post-Pliocene establishment of the present monsoonal climate in SW China: evidence from the late Pliocene Longmen megaflora. Clim. Past 9, 1911–1920.
Sun, X.-J., Wang, P.X., 2005. How old is the Asian monsoon system? — palaeobotanical records from China. Palaeogeogr. Palaeoclimatol. Palaeoecol. 222, 181–222.
Sun, B.-N., Wu, J.-Y., Christopher, Y.S., Ding, S.T., Li, X.C., Xie, S.P., Yan, D.F., Lin, Z.C., 2011. Reconstructing Neogene vegetation and climates to infer tectonic uplift in western Yunnan, China. Palaeogeogr. Palaeoclimatol. Palaeoecol. 304, 328–336.
Tao, J.-R., 1986. Neogene flora of Lanping and its significance in middle watershed of Selween–Mekong–Yangtze Rivers. In: Tao, J.-R. (Ed.), Hengduan Mountain Investigation Special. Science and Technology Publishing House, Beijing, pp. 58–65.
Uhl, D., Klotz, S., Traiser, C., Thiel, C., Utescher, T., Kowalski, E., Dilcher, D.L., 2007. Cenozoic paleotemperatures and leaf physiognomy—a European perspective. Palaeogeogr. Palaeoclimatol. Palaeoecol. 248, 24–31.
Utescher, T., Mosbrugger, V., 2013. The Palaeoflora Database. <http://www.palaeoflora.de>.
Utescher, T., Mosbrugger, V., Ashraf, A.R., 2000. Terrestrial climate evolution in Northwest Germany over the last 25 million years. Palaios 15, 430–449.
Utescher, T., Bruch, A.A., Micheels, A., Mosbrugger, V., Popova, S., 2011. Cenozoic climate gradients in Eurasia—a palaeo-perspective on future climate change? Palaeogeogr. Palaeoclimatol. Palaeoecol. 304, 351–358.
Utescher, T., Bruch, A.A., Erdei, B., François, L., Ivanov, D., Jacques, F.M.B., Kern, A.K., Liu, Y.-S., Mosbrugger, V., Spicer, R.A., 2014. The Coexistence Approach—Theoretical background and practical considerations of using plant fossils for climate quantification. Palaeogeogr. Palaeoclimatol. Palaeoecol. 410, 58–73.
Wang, Y., 2006. Yunnan Mountain Climate. Yunnan Science Press, Kunming, 412 pp (in Chinese).
Wang, W.-M., Shu, J.-W., 2004. Late Cenozoic palynofloras from Qujing Basin, Yunnan, China. Acta Palaeontologica Sinica 43, 254–261 (in Chinese with English abstract).
Wang, S.-Y., Zhang, W., 2002. Yunnan Geography. Yunnan Nationalities Publishing House, Kunming, pp. 33–83 (in Chinese).
Westaway, R., 2009. Active crustal deformation beyond the SE margin of the Tibetan Plateau: constraints from the evolution of fluvial systems. Global Planet. Change 68, 395–417.
Writing Group of Yunnan Regional Geological Stratigraphy (WGYRGS), 1978. Regional Geological Stratigraphy in Southwest China: Yunnan. Geological Publishing House, Beijing, 255 pp (in Chinese).
Williams, H., Turner, S., Kelley, S., Harris, N., 2001. Age and composition of dikes in southern Tibet: new constraints on the timing of east-west extension and its relationship to postcollisional volcanism. Geology 29, 339–342.
Wu, M.-C., Chan, J.C.L., 1997. Upper-level features associated with winter Monsoon surges over South China. Mon. Weather Rev. 125, 317–340.
Xie, S., Sun, B., Wu, J., Lin, Z., Yan, D., Xiao, L., 2012. Palaeoclimatic estimates for the late Pliocene based on leaf physiognomy from western Yunnan, China. Turk. J. Earth Sci. 21, 251–261.
Xu, J.-X., 2002. Palynology, Paleovegetation and Paleoclimate of Neogene, Central-Western Yunnan, China. Ph.D. Thesis, Institute of Botany, the Chinese Academy of Sciences, Beijing, China (in Chinese with English abstract).
Xu, J.-X., Wang, Y.-F., Du, N.-Q., 2003. Late Pliocene vegetation and palaeoclimate of Yangyi and Longling of western Yunnan Province. J. Palaeogeogr. 5, 218–224 (in Chinese with English abstract).
Xu, J.-X., Ferguson, D.K., Li, C.-S., Wang, Y.-F., Du, N.-Q., 2004. Climatic and ecological implications of late Pliocene palynoflora from Longling, Yunnan, China. Quatern. Int. 117, 91–103.
Xu, L., Zhou, S., Bao, D., 2008. Influences of tectonic uplift and climate changes on Yazheku River terraces in the eastern Tibetan Plateau. Acta Geol. Sinica 82, 269–280.
Yao, Y.-F., Bruch, A.A., Cheng, Y.-M., Mosbrugger, V., Wang, Y.-F., Li, C.-S., 2012. Monsoon versus uplift in southwestern China—Late Pliocene climate in Yuanmou Basin, Yunnan. PloS ONE 7, e37760.
Yunnan Bureau of Geology and Mineral Resources (YBGMR), 1990. Regional Geology of Yunnan Province. Geological Publishing House, Beijing, 743 pp (in Chinese).
Yunnan Meteorological Bureau, 1984. Agricultural Climate Database of Yunnan. Yunnan People's Press, Kunming, 240 pp (in Chinese).
Zachos, J., Pagani, M., Sloan, L., Thomas, E., Billups, K., 2001. Trends, rhythms, and aberrations in global climate 65 Ma to present. Science 292, 686–693.
Zhang, J.-J., Ding, L., 2003. East west extension in Tibetan Plateau and its significance to tectonic evolution. Chin. J. Geol. 2, 179–189 (in Chinese with English abstract).
Zhang, H.-P., Liu, S.-F., Yang, H., Zhang, Y.-Q., Zhang, G.-W., 2006. Geomorphic characteristics of the Minjiang drainage basin (eastern Tibetan Plateau) and its tectonic implications: New insights from a digital elevation model study. Island Arc 15, 239–250.
Zhang, Q.-Q., Ferguson, D.K., Mosbrugger, V., Wang, Y.-F., Li, C.-S., 2012. Vegetation and climatic changes of SW China in response to the uplift of Tibetan Plateau. Palaeogeogr. Palaeoclimatol. Palaeoecol. 363–364, 23–36.
Zheng, H., Powell, C.M., Rea, D.K., Wang, J., Wang, P., 2004. Late Miocene and mid-Pliocene enhancement of the East Asian monsoon as viewed from the land and sea. Global Planet. Change 41, 147–155.
Zhou, Z.-K., 2000. The late Pliocene Miyi flora. In: Tao, J.-R. (Ed.), The Evolution of the Late Cretaceous-Cenozoic Floras in China. Science Press, Beijing, pp. 40–49 (in Chinese).